Spectroscopic analysis of small organic molecules: A comprehensive near-edge x-ray-absorption fine-structure study of C_6-ring-containing molecules

C. Kolczewski[a)]
Fritz-Haber-Institut der Max-Planck-Gesellschaft, Faradayweg 4-6, 14195 Berlin, Germany

R. Püttner and M. Martins[b)]
Freie Universität Berlin, Institut für Experimentalphysik, Arnimallee 14, 14195 Berlin, Germany

A. S. Schlachter
Advanced Light Source, Lawrence Berkeley National Laboratory, Berkeley, California 94720

G. Snell
Advanced Light Source, Lawrence Berkeley National Laboratory, Berkeley, California 94720 and Department of Physics, Western Michigan University, Kalamazoo, Michigan 49008-5151

M. M. Sant'Anna[c)]
Advanced Light Source, Lawrence Berkeley National Laboratory, Berkeley, California 94720

K. Hermann
Fritz-Haber-Institut der Max-Planck-Gesellschaft, Faradayweg 4-6, 14195 Berlin, Germany

G. Kaindl
Freie Universität Berlin, Institut für Experimentalphysik, Arnimallee 14, 14195 Berlin, Germany

(Received 1 August 2005; accepted 28 October 2005; published online 18 January 2006)

We report high-resolution C 1*s* near-edge x-ray-absorption fine-structure (NEXAFS) spectra of the C_6-ring-containing molecules benzene (C_6H_6), 1,3- and 1,4-cyclohexadiene (C_6H_8), cyclohexene (C_6H_{10}), cyclohexane (C_6H_{12}), styrene (C_8H_8), and ethylbenzene (C_8H_{10}) which allow us to examine the gradual development of delocalization of the corresponding π electron systems. Due to the high experimental resolution, vibrational progressions can be partly resolved in the spectra. The experimental spectra are compared with theoretical NEXAFS spectra obtained from density-functional theory calculations where electronic final-state relaxation is accounted for. The comparison yields very good agreement between theoretical spectra and experimental results. In all cases, the spectra can be described by excitations to π^*- and σ^*-type final-state orbitals with valence character, while final-state orbitals of Rydberg character make only minor contributions. The lowest C $1s \rightarrow 1\pi^*$ excitation energy is found to agree in the (experimental and theoretical) spectra of all molecules except for 1,3-cyclohexadiene (C_6H_8) where an energy smaller by about 0.6 eV is obtained. The theoretical analysis can explain this result by different binding properties of this molecule compared to the others. © *2006 American Institute of Physics*. [DOI: 10.1063/1.2139674]

I. INTRODUCTION

Near-edge x-ray-absorption fine-structure (NEXAFS) spectroscopy is a powerful tool for probing the electronic structure of unoccupied orbitals and bands in molecules,[1–4] in adsorbate systems,[5–8] and in solids.[9–11] Here element-specific ionization potentials of the core-level region allow an unambiguous identification of individual atoms or atom groups in complex systems. In addition, useful information about local coordination and binding can be obtained as well as—in the case of adsorbate systems—molecular adsorbate geometry. Small organic molecules are of particular interest for NEXAFS spectroscopy since they are used as model compounds for building blocks in large biological systems[12,13] and in polymers of industrial relevance.[14–16] This is based on the experience that specific features observed in NEXAFS spectra of model compounds are reproduced in the spectra of more complex systems (building-block principle).[17–19] The building-block principle is particularly suitable for systems where the intermolecular coupling between the subsystems is weak and its influence on spectral properties is small compared with those of the separate subsystems. Therefore, a detailed analysis of model compound spectra is essential for an understanding of the spectra of complex molecules such as peptides or polymers.[12,20]

Many organic molecules, which can act as building blocks, are described in parts of their electronic structure by conjugated double bonds resulting in a delocalized π electron system. Details of the π electron system determine im-

[a)]Electronic mail: kolczew@fhi-berlin.mpg.de
[b)]Present address: Universität Hamburg, Institut für Experimentalphysik, Luruper Chaussee 149, D-22761 Hamburg, Germany.
[c)]Present address: Instituto de Fisica, Universidade Federal do Rio de Janeiro, Caixa Postal 68528, Rio de Janeiro, RJ 21941-972, Brazil.

portant molecular properties, such as color, magnetism, or chemical reactivity. Combining these molecules as building blocks to form larger complexes may influence their π electron system significantly and, as a consequence, may lead to significant modifications of details in the NEXAFS spectra of the larger complex.[13] Thus, it is important to study NEXAFS spectra of akin molecules with different types of π bonds in order to enable an interpretation of changes in the delocalized π system reflected in the NEXAFS spectra. Small hydrocarbon molecules facilitate this comparison in many cases since, in these systems, electronic core transitions to unoccupied π^* levels are well separated energetically from other excitations, as will be shown below.

In this paper we present high-resolution NEXAFS spectra of a series of small cyclic hydrocarbon molecules, C_6H_n (n=6, 8, 10, 12) and C_8H_n (n=8, 10) in gas phase, where the experimental spectra are compared with theoretical spectra obtained from density-functional theory (DFT) calculations. Based on our theoretical studies we are able to assign the spectral features in the experimental spectra. Further, the present selection of molecules enables us to examine the gradual development of a delocalized π electron system in the C_6 ring and its spectroscopic consequences which may be used as fingerprints of the molecular components in larger molecules. Finally, the experimental high-resolution spectra show pronounced contributions stemming from vibrational excitations which can be accounted for by an *ad hoc* approach yielding remarkably good agreement.

In Sec. II we describe experimental details while Sec. III deals with theoretical approaches and computational methods used in this work. Section IV discusses the experimental data and compares with theoretical results. Finally, in Sec. V we summarize our conclusions.

II. EXPERIMENTAL DETAILS

NEXAFS spectra of the cyclic hydrocarbon molecules, C_6H_n (n=6, 8, 10, 12) and C_8H_n (n=8, 10), were recorded at the undulator beam line 10.0.1 of the Advanced Light Source (ALS), Berkeley, which is equipped with a spherical-grating monochromator. All spectra were obtained by measuring the total photoionization yield with a gas cell that contains two parallel plates with lengths of 10 cm for the collection of the charged particles resulting from photoionization, where a voltage of 100 eV was applied to accelerate the particles towards the plates. The photoionization cell was filled with approximately 35 μbars of the measured gas and was separated from the ultrahigh vacuum of the monochromator by a 1000-Å-thick aluminum window. In order to avoid the accumulation of impurities in the form of fragmentation products formed by deexcitation processes in the gas the spectra were measured at constant flow through the gas cell. With this setup the measured spectra did not change with time, ensuring the absence of dissociation products. The estimated resolution of all spectra amounts to about 65 meV.

The spectra measured at beam line 10.0.1 were calibrated by shifting the nominal energy positions of the prominent C $1s \rightarrow \pi^*$ transitions to the calibrated values obtained from the medium-resolution spectra that had been measured previously at the plane-grating monochromator SX700/II at BESSY in Berlin. The latter spectra were calibrated using the well-known energy position of the $\nu''=0 \rightarrow \nu'=0$ transition of the N $1s \rightarrow \pi^*$ excitation in N_2 at 400.88 eV,[21] together with the relation $\Delta E \propto E^{3/2}$ valid for plane-grating monochromators. (ΔE describes the difference between the measured and the actual energy position.) This procedure yields an accuracy in the energy positioning of better than 30 meV for benzene (C_6H_6), styrene (C_8H_8), and ethylbenzene (C_8H_{10}) while for cyclohexadiene (C_6H_8) the accuracy is estimated to be smaller than 50 meV and for cyclohexene (C_6H_{10})/cyclohexane (C_6H_{12}) smaller than 100 meV. To put the results on a common basis we have listed experimental excitation energies obtained from peak maxima only with one digit accuracy.

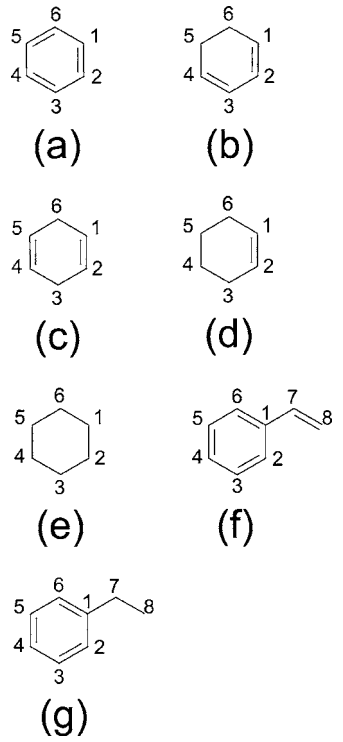

FIG. 1. Schematic drawings of the hydrocarbon molecules (a) benzene (C_6H_6), (b) 1,3-cyclohexadiene (C_6H_8), (c) 1,4-cyclohexadiene (C_6H_8), (d) cyclohexene (C_6H_{10}), (e) cyclohexane (C_6H_{12}), (f) styrene (C_8H_8), and (g) ethylbenzene (C_8H_{10}). The numbers inside the drawings refer to labels of the carbon atoms used in this work.

III. THEORETICAL DETAILS

The electronic ground states of the hydrocarbon molecules, C_6H_n (n=6, 8, 10, 12) and C_8H_n (n=8, 10), see Fig. 1, as well as corresponding core electron excitations, yielding theoretical NEXAFS spectra, are obtained from quantum-chemical calculations. Here we apply DFT together with the gradient-corrected RPBE exchange/correlation functional[22,23] as implemented in the STOBE computer code.[24] This code is based on linear combinations of atomic Gaussian basis sets where we use an all-electron triple-zeta valence plus polarization (TZVP) set in a $[4s,3p]$ contraction with one added d function for carbon[25] and a primitive $(5s)$ set augmented with one p function and contracted to $[3s,1p]$ for

hydrogen.[26] In the calculations of carbon core electron excitations the orbital basis of the corresponding ionization center is of all-electron IGLO-III quality[27] yielding an improved representation of relaxation effects in the inner atomic shells. For the remaining carbon centers effective core potentials[28] (ECPs) describing the C 1*s* core and appropriate valence basis sets are applied. The use of ECPs simplifies the identification of the core hole orbital while it has only negligible effects on the computed excitation spectrum, see Ref. 29. This treatment assumes a localized core hole in the description of the excitation. In this context, the problem of localized versus delocalized core holes has been discussed extensively in the literature[30–33] where we adopt the view of Fink *et al.* in their previous studies on ethene.[32] Finally, the present calculations of carbon core electron excitations include a large diffuse even-tempered $[19s,19p,19d]$ basis set[34] located at the excitation center which accounts for unbound resonance wave functions within the core electron region (double basis-set technique[34]).

In an initial step, geometry optimizations are carried out for the electronic ground states of all molecules to yield corresponding equilibrium geometries. The results are provided as supplementary information in EPAPS.[35] For styrene, a planar geometry was obtained, which is in contrast to previous studies suggesting[36] that the vinyl group of C_8H_8 is rotated by 27° with respect to the C_6-ring plane.[36] We have calculated the NEXAFS spectra for both geometries and find only very small differences. Therefore, we use the planar geometry in the following. The molecular equilibrium geometries are then used in calculations on C 1*s* core excitations originating at all nonequivalent carbon atoms in each molecule. In a first calculation the complete excitation spectrum of each molecule is evaluated using Slater's transition state (TS) method[37,38] in combination with the above-mentioned double basis-set technique[34] yielding excitation energies and dipole transition moments.

The DFT TS calculations assume a frozen molecular ion density and thus neglect electronic relaxation on the molecular ion core upon adding the excited electron. For the present molecules this effect is largest for the valencelike π^* excitations. Therefore, in a second step these and other most prominent excitations of each spectrum, referring to largest dipole transition moments, are reevaluated by ΔKohn-Sham (ΔKS) DFT calculations to obtain more accurate excitation energies which reflect the correct amount of electronic relaxation connected with the excitation process. For all other excitations relaxation is accounted for in a more approximate way by correcting their energies by the difference of the ionization potential (IP) evaluated with the TS method and the corresponding value from ΔKS calculations. Further, the excitation spectrum is corrected by a rigid shift of 0.2 eV to higher energies to account for relativistic effects contributing to core excitation.[39] The improved discrete excitation spectrum is then subjected to a Gaussian convolution with an energy-dependent broadening to arrive at a theoretical spectrum to be compared with NEXAFS experiments. In the energy region below ionization threshold the broadening [full width at half maximum (FWHM)] was set to 0.2 eV while a linear increase up to a width of 4.5 eV was assumed for higher energies, as is common practice in the analysis of experimental NEXAFS spectra.[40]

The experimental high-resolution spectra presented in this work show pronounced contributions due to vibrational excitations. However, it is quite difficult and technically complex to include vibrational fine structure in the theoretical treatment.[41,42] Therefore, we consider an *ad hoc* approach by including, for each transition, the vibrational fine structure obtained experimentally for excitations originating at atoms in a similar binding environment. This approach has been applied successfully to explain differences in intensities between the experimental and theoretical spectra of pyridine in the region of C $1s \rightarrow 1\pi^*$ excitations.[40] For the present series of small organic molecules we find also remarkably good agreement between the experimental NEXAFS spectra and our theoretical results using this *ad hoc* approach to include vibrational fine structure.

IV. RESULTS AND DISCUSSION

A. Assignment of spectral features

Figure 2 compares experimental and theoretical NEXAFS spectra of the hydrocarbon molecules C_6H_n ($n=6$, 8, 10, 12) where prominent peaks are labeled accordingly. Experimental excitation energies are obtained from maxima of corresponding peaks, avoiding a full vibrational analysis which is beyond the scope of this work. The theoretical spectra of Fig. 2(B) are obtained from transition state calculations described in Sec. III where ΔKS corrections for the ionization energies and for all prominent excitations as well as relativistic corrections are included. The experimental spectrum of **benzene** shown in Fig. 2(A)(a) is characterized by four peak structures A–D which are reproduced quite well in the theoretical spectrum in Fig. 2(B)(a). The peak assignment based on final-state orbitals, see Table Ia, has recently been discussed in detail[43] and will be summarized only briefly in the following. Peaks A and D are assigned to excitations to the unoccupied π^* orbitals of e_{2u} and b_{2g} symmetries in D_{6h} notation (b_1 in C_{2v} notation which refers to the correct symmetry of the molecule with a localized C 1*s* core hole). Peak D includes also minor contributions of excitations to rather diffuse Rydberg orbitals. Peaks B and C have been assigned to different excitations in the literature.[43] Our recent analysis[43] yields an assignment to excitations to σ-type final-state orbitals with σ^* (C–C) (peak B) and σ^* (C–H) (peak C) valence character and only minor Rydberg orbital admixing, see Fig. 3. This assignment is supported by the mean-squared radii $\langle r^2 \rangle$ of the corresponding final-state orbitals given in Table II. These values are all relatively small, indicating "compact" orbitals of dominant valence character, whereas diffuse Rydberg orbitals are characterized by larger $\langle r^2 \rangle$ values (typically >100 Å^2, depending on the size of the molecule[44]). Interestingly, transitions involving these two final-state orbitals are found in all hydrocarbon compounds considered in this work. Thus, we conclude that these transitions can be taken as fingerprints for carbon 6-ring-containing molecules. Despite the admixing of diffuse Ryd-

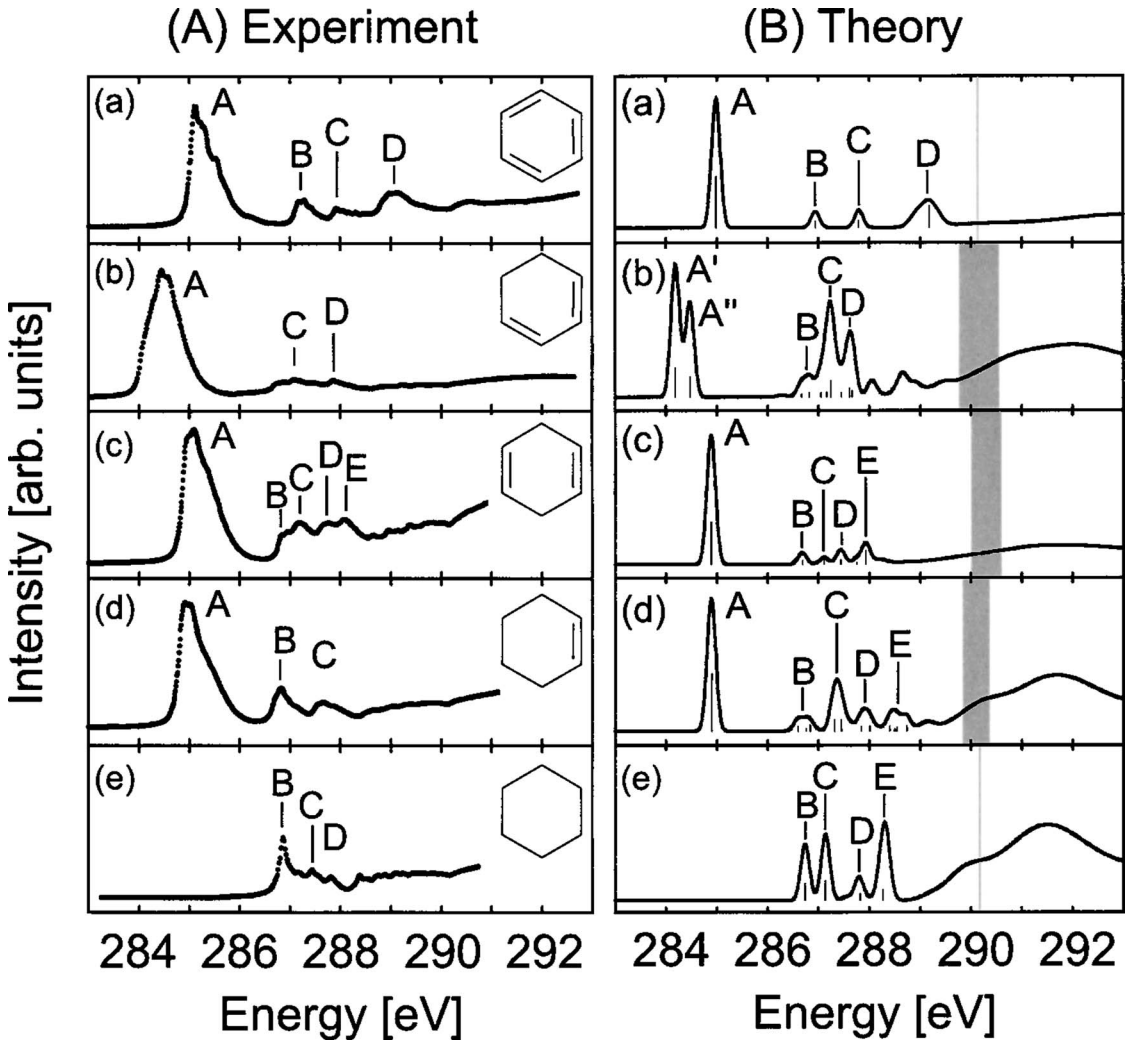

FIG. 2. NEXAFS spectra of the hydrocarbon molecules C_6H_n (n=6, 8, 10, 12) near the C 1s ionization threshold. (A) Experimental spectra for (a) benzene (C_6H_6), (b) 1,3-cyclohexadiene (C_6H_8), (c) 1,4-cyclohexadiene (C_6H_8), (d) cyclohexene (C_6H_{10}), and (e) cyclohexane (C_6H_{12}) and (B) theoretical spectra for the corresponding molecules. Prominent peaks in the spectra are labeled A–D. The theoretical spectra include calculated excitation energies by the small thin vertical lines and ionization energy ranges are indicated by the gray areas or lines.

berg character to the two final-state orbitals we will refer to them in the following by σ^* (C–C) and σ^* (C–H).[43]

Cyclohexadiene appears as two different isomers, 1,3-cyclohexadiene and 1,4-cyclohexadiene, differing by the location of the C═C double bonds, see Fig. 1. The experimental spectrum of **1,3-cyclohexadiene** in Fig. 2(A)(b) shows a broad asymmetric peak A at 284.4 eV and some weaker peaks above 286.6 eV. Based on our theoretical analysis, peak A can be assigned to C $1s \rightarrow 1\pi^*$ excitations originating at all carbon atoms with double bonds. These excitations resemble those characterizing the lowest excitation peak A of benzene. However, the energy position of peak A in 1,3-cyclohexadiene is found to be lower by about 0.6 eV compared to that of benzene, which will be discussed in Sec. IV C. The theoretical NEXAFS spectrum of 1,3-cyclohexadiene given in Fig. 2(B)(b), see also Table Ib, shows a two-peak structure, peaks A′ at 284.17 eV and A″ at 284.47 eV, in the energy range of the experimental peak A. The two theoretical peaks refer to C $1s \rightarrow 1\pi^*$ excitations originating at different carbon atoms. Excitations originating at C1 and C4, which are bound to one CH and one CH_2 group, are lower in energy (peak A′) than those originating at C2 and C3, bound to two CH groups (peak A″). Altogether, the double-peak structure of the theoretical spectrum can explain the asymmetric peak A found experimentally if vibrational broadening of the peak is taken into account, see Sec. IV E. The theoretical NEXAFS spectrum of Fig. 2(B)(b) also exhibits additional peaks B–D above 287 eV. Peak B is assigned to transitions originating at carbon atoms C1, C2, C3, and C4 with final-state orbitals of σ^* (C–C) character. Peak C is due to C $1s \rightarrow 2\pi^*$ transitions at C1, C2, C3, and C4 as well as to transitions originating at C5 and C6 with final-state orbitals of σ^* (C–C) character. Finally, peak D is determined by transitions to final-state orbitals with σ^* (C–H) character and some Rydberg admixture for all C atoms. For further details see Table Ib. Note the change in the energetic order of the excited-state orbitals from σ^* (C–C), σ^* (C–H), and π^* in benzene to σ^* (C–C), π^*, and σ^* (C–H) in 1,3-cyclohexadiene. This difference is explained analogous to the shift of the $1\pi^*$ orbital discussed in Sec. IV C. The peak region above 287 eV also appears in the experimental NEXAFS spectrum in Fig. 2(A)(b), however, with

TABLE I. Excitation energies obtained from the experimental and theoretical NEXAFS spectra for C_6H_n (n=6, 8, 10, 12). The excitation peaks are labeled according to their energetic sequence, see Fig. 2, where corresponding energies (given in eV) are denoted as E_{exp} and E_{th}, respectively. Experimental excitation energies are obtained from the maxima of corresponding peaks, see text. The peak assignment "excitation" is based on the calculated excitations and characterized by the carbon atom of the 1s core hole (C1–C6, see Fig. 1) as well as the final-state orbital character. All theoretical spectra include relaxation and relativistic effects. Final-state orbitals are denoted by double quotes, e.g., "σ^* (C–C)," if the assignment refers only to the major component of an orbital mixture. (a) Benzene, (b) 1,3-cyclohexadiene, (c) 1,4-cyclohexadiene, (d) cyclohexene, and (e) cyclohexane.

(a) Peak	E_{exp} (eV)	E_{th} (eV)	Excitation (C1–C6) →
A	285.1	284.98	$1\pi^*$
B	287.2	286.94	σ^* (C–C)
C	287.9	287.79	σ^* (C–H)
D	289.1	289.18	$3\pi^*$
(b) Peak	E_{exp} (eV)	E_{th} (eV)	Excitation core→final
A′	284.4	284.17	(C2,3)→$1\pi^*$
A″	⋯	284.47	(C1,4)→$1\pi^*$
B	⋯	286.64	(C2,3)→σ^* (C–C)
B	⋯	286.81	(C1,4)→σ^* (C–C)
C	287.1	287.02	(C5,6)→σ^* (C–C)
C	⋯	287.14	(C2,3)→$2\pi^*$
C	⋯	287.24	(C1,4)→$2\pi^*$
D	287.9	287.40	(C2,3)→σ^* (C–H)
D	⋯	287.59	(C5,6)→σ^* (C–H)
D	⋯	287.65	(C1,4)→σ^* (C–H)
(c) Peak	E_{exp} (eV)	E_{th} (eV)	Excitation core→final
A	285.1	284.88	(C1,2,4,5)→$1\pi^*$
B	286.9	286.67	(C1,2,4,5)→σ^* (C–C)
C	287.2	287.12	(C3,6)→σ^* (C–C)
D	287.8	287.43	(C1,2,4,5)→σ^* (C–H)
E	288.1	287.73	(C1,2,4,5)→$2\pi^*$
E	⋯	287.95	(C1,2,4,5)→$2\pi^*$ (C3,6)→"π^*"
(d) Peak	E_{exp} (eV)	E_{th} (eV)	Excitation core→final
A	284.9	284.88	(C1,2)→$1\pi^*$
B	286.8	286.58	(C1,2)→σ^* (C–C)
B	⋯	286.75	(C3,6)→"σ^* (C–C)"
B	⋯	286.83	(C4,5)→"σ^* (C–C)"
C	287.7	287.30	(C1,2)→σ^* (C–H)
C	⋯	287.30	(C3,6)→?
C	⋯	287.44	(C4,5)→?
D	⋯	287.85	(C3,6)→"σ^* (C–H)"
D	⋯	287.99	(C4,5)→"σ^* (C–H)"
E	⋯	288.39	(C3,6)→?
E	⋯	288.48–288.73	(C4,5)→?
(e) Peak	E_{exp} (eV)	E_{th} (eV)	Excitation (C1–6)→
B	286.8	286.72	σ^* (C–C)
C	287.4	287.12	"σ^* (C–C)"
D	287.8	287.82	"σ^* (C–H)"
E	⋯	288.27	"σ^* (C–H)"

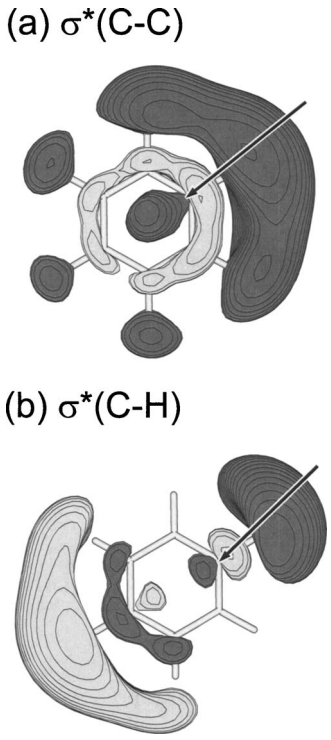

FIG. 3. Constant-value surface plots of final-state orbitals of benzene evaluated in the presence of the C 1s core hole. (a) σ^* (C–C) orbital (peak B in the spectrum) and (b) σ^* (C–H) orbital (peak C). The molecular structure is sketched by the bond sticks. The arrows indicate the position of the ionized carbon atom.

greatly reduced intensity, which will be discussed separately in Sec. IV D.

The experimental spectrum of **1,4-cyclohexadiene** in Fig. 2(A)(c) shows its most prominent peak A at 285.1 eV which is comparable with the excitation energy of peak A for benzene. In addition, smaller peaks B–E appear between 287 and 288 eV. The experimental spectrum is reproduced well by theory, as shown in Fig. 2(B)(c), see Table Ic. As before, peak A is assigned to C $1s \rightarrow 1\pi^*$ transitions originating at the double-bonded carbon atoms C1, C2, C4, and C5. Transitions to final-state orbitals with σ^* (C–C) character contribute to peak B (originating at C1, C2, C4, and C5) and peak C (originating at C3 and C6), respectively. Peak D is assigned to transitions to final-state orbitals with mixed σ^* (C–H) character originating at C1, C2, C4, and C5. Finally, peak E is due to C $1s \rightarrow 2\pi^*$ transition at any of the C atoms.

The experimental spectrum of **cyclohexene** in Fig. 2(A)(d) is also dominated by a prominent peak at 284.9 eV (peak A), along with less intense features at 286.8 and 287.7 eV (peaks B and C). These peaks are accounted for by the

TABLE II. Mean-squared radii $\langle r^2 \rangle$ of final-state orbitals for the four most prominent transitions of benzene as obtained from the transition state calculations, see text. All values are given in Å^2.

Peak	Excitation (C1–C6) →	Mean-squared radii $\langle r^2 \rangle$
A	$1\pi^*$	18.56
B	σ^*(C–C)	46.29
C	σ^*(C–H)	77.56
D	$3\pi^*$	43.72

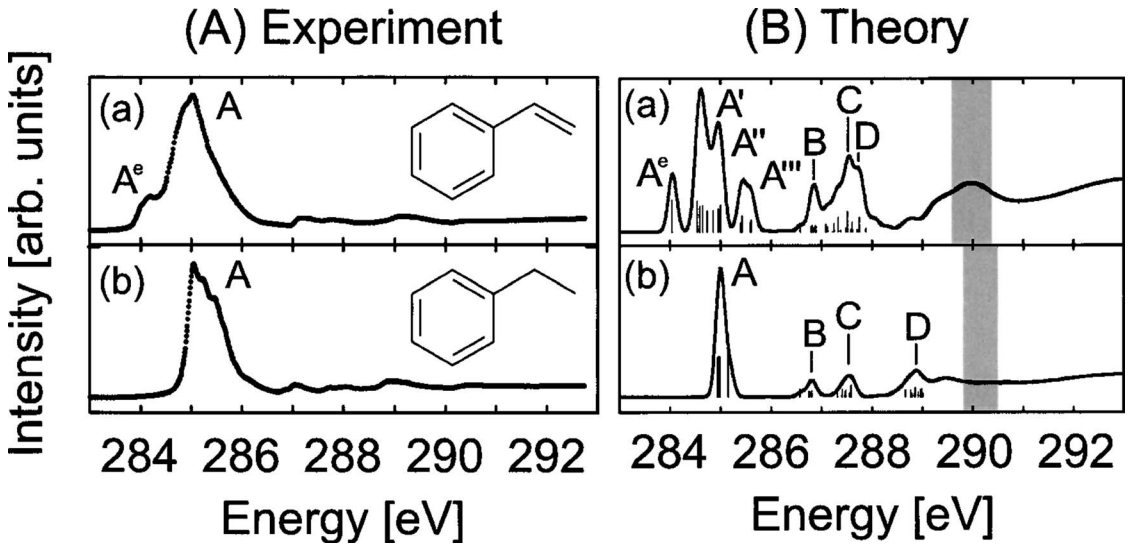

FIG. 4. NEXAFS spectra of the hydrocarbon molecules C_8H_n ($n=8$, 10) near the C 1*s* ionization threshold. (A) Experimental spectra for (a) styrene (C_8H_8) and (b) ethylbenzene (C_8H_{10}) and (B) theoretical spectra for the corresponding molecules. Prominent peaks in the spectra are labeled A–D. The theoretical spectra include calculated excitation energies by the small thin vertical lines and ionization energy ranges are indicated by the gray areas or lines.

theoretical spectrum given in Fig. 2(B)(d), see Table Id. As before, peak A is due to C $1s \rightarrow 1\pi^*$ transitions originating at double-bonded carbon atoms C1 and C2, see Fig. 1(d), while the other ring atoms C3–C6 do not contribute. Peak B is assigned to final-state orbitals with σ^* (C–C) character originating at all C atoms. The assignment for peaks C–E is more involved. There are considerable contributions from C1, C2 $1s \rightarrow \sigma^*$ (C–H) transitions as well as from transitions originating at the other carbon atoms to more complex final-state orbitals. Peak D can be characterized by C3–C6 $1s \rightarrow \sigma^*$ (C–H) transitions. As a consequence of the nonplanar geometry of the C_6 ring in cyclohexene, the assignment at higher excitation energies is less obvious. Thus, for peak E, no clear assignment can be made. Note that there is only one π^* orbital in this molecule due to only one double bond.

The experimental spectrum of **cyclohexane** in Fig. 2(A)(e) does not exhibit a peak in the energy region about 285 eV which, compared with peaks A of the previous spectra, can be attributed to missing C═C double bonds in this molecule. The lowest (prominent) peak B lies at 286.8 eV, followed by two smaller peaks C and D at 287.4 and 287.8 eV, respectively. These peaks are reproduced by the theoretical spectrum given in Fig. 2(B)(e), see also Table Ie. Peak B is attributed to excitations to final-state orbitals having σ symmetry. Further, peaks C–E are all assigned to transitions to final-state orbitals with mixed valence/Rydberg character. A more detailed analysis is difficult due to very diffuse character of these orbitals.

Figure 4 compares experimental and theoretical NEXAFS spectra of the hydrocarbon molecules C_8H_n ($n=8$, 10), where prominent peaks are labeled accordingly. The experimental spectrum of **styrene** in Fig. 4(A)(a) is dominated by a broad and structureless peak A at about 285 eV with a small low-energy shoulder at 284.2 eV labeled A^e. In addition, there are peaks of rather small intensity between 287 and 290 eV. The corresponding theoretical NEXAFS spectrum, see Fig. 4(B)(a) and Table IIIa, is consistent with the experimental spectrum. All transitions contributing to peaks A^e, A′, A″, and A‴ are assigned to C $1s \rightarrow \pi^*$ transitions. In a first approximation, the π^* orbitals of styrene are described by linear combinations of those of benzene and ethylene. The self-consistent calculations yield three lowest unoccupied π^* orbitals, as shown in Fig. 5, while the higher-lying empty orbitals are too diffuse to be included in this figure. The experimental low-energy shoulder A^e is reproduced by theory as a separate peak A^e and assigned to a transition from the C8 atom of C_8H_8, see Fig. 1, to the $1\pi^*$ orbital whose shape is shown as an isosurface plot in Fig. 5(a) Since C8 is the only carbon atom with three C–H bonds, it can attract more electrons from hydrogen than the other carbon atoms. This increased negative charge of C8 can explain the observed lower excitation energy of peak A^e in terms of a chemical shift, which is also observed for the ionization energies in Table IV. Note that the present explanation differs from that given by Wühn *et al.*[45] who assigned the shoulder A^e to excitations originating from both side-chain atoms, C7 and C8.

The higher-lying peaks A′, A″, and A‴ of the theoretical NEXAFS spectrum of styrene result in the broad asymmetric peak A of the experimental spectrum if vibrational progression, not accounted for in the theoretical spectrum, is considered. The peaks result from numerous excitations as indicated by the vertical lines in Fig. 4(B)(a). Contributions to peak A′ refer to transitions originating at C7, the *ortho*-(C2 and C6), and *para*-(C4) carbon atoms of the C_6 ring to the $1\pi^*$ final-state orbital. Peak A″ is due to excitations from the *meta*-(C3 and C5) and *ipso*-(C1) atoms of the C_6 ring to the same $1\pi^*$ orbital. Peak A‴ is assigned to transitions to the $2\pi^*$ orbital, see Fig. 5(b), originating at C2, C3, C5, and C6. Peaks B–D of the theoretical spectrum are also composed of many different excitations due to the eight nonequivalent carbon atoms as summarized in Table IIIa. Transitions contributing to peak B are mainly assigned to final-state orbitals with σ^* (C–C) character. Peak C is due to final-state orbitals of mixed σ^* (C–C) and Rydberg character, mixed σ^* (C–H) and Rydberg character, and of $3\pi^*$ character [Fig. 5(c)]. Fi-

TABLE III. Excitation energies obtained from the experimental and theoretical NEXAFS spectra for C_8H_n (n=8, 10), as shown in Fig. 4. For further details, see Table I (a) styrene and (b) ethylbenzene.

(a) Peak	E_{exp} (eV)	E_{th} (eV)	Excitation core→final
A[e]	284.2	284.02	(C8)→1π^*
A′	⋯	284.53	(C7)→1π^*
A′	⋯	284.59	(C2)→1π^*
A′	⋯	284.67	(C4)→1π^*
A′	⋯	284.75	(C6)→1π^*
A″	285.0	284.88	(C5)→1π^*
A″	⋯	284.94	(C1)→1π^*
A″	⋯	285.02	(C3)→1π^*
A‴	⋯	285.42	(C3)→2π^*
A‴	⋯	285.44	(C6)→2π^*
A‴	⋯	285.59	(C2)→2π^*
A‴	⋯	285.62	(C5)→2π^*
B	⋯	286.56	(C8)→"σ^* (C–C) vinyl"
B	⋯	286.80	(C8)→"σ^* (C–C) vinyl"
B	⋯	286.82	(C4)→σ^* (C–C)
B	⋯	286.85	(C2)→σ^* (C–C)
B	⋯	286.89	(C3)→σ^* (C–C)
B	⋯	286.91	(C5)→σ^* (C–C)
C	⋯	287.06	(C8)→3π^*
C	⋯	287.14	(C6)→σ^* (C–C)
C	⋯	287.22	(C7)→2π^*
C	⋯	287.24	(C7)→σ^* (C–C) vinyl
C	⋯	287.35	(C4)→3π^*
C	⋯	287.36	(C8)→σ^* (C–C) ring
C	⋯	287.49	(C6)→σ^* (C–H)
C	⋯	287.51	(C6)→3π^*
C	⋯	287.51	(C7)→3π^*
C	⋯	287.52	(C2)→σ^* (C–H)
C	⋯	287.60	(C5)→"σ^* (C–H)"
C	⋯	287.62	(C5)→3π^*
C	⋯	287.64	(C3)→"σ^* (C–H)"
D	⋯	287.71	(C7)→"σ^* (C–H)"
D	⋯	287.73	(C1)→3π^*
D	⋯	287.73	(C4)→"σ^* (C–H)"
D	⋯	287.74	(C8)→?
D	⋯	287.77	(C3)→3π^*
D	⋯	287.87	(C8)→?

(b) Peak	E_{exp} (eV)	E_{th} (eV)	Excitation core→final
A	285.1	284.95	(C2,6)→1π^*
A	⋯	284.99	(C3,5)→1π^*
A	⋯	284.99	(C4)→1π^*
A	⋯	285.14	(C1)→1π^*
B	⋯	286.60	(C8)→1π^*+ ethyl
B	⋯	286.76	(C4)→σ^* (C–C)
B	⋯	286.76	(C2,6)→σ^* (C–C)
B	⋯	286.81	(C3,5)→σ^* (C–C)
C	⋯	287.35	(C8)→?
C	⋯	287.42	(C7)→?
C	⋯	287.47	(C2,6)→σ^* (C–H)
C	⋯	287.52	(C8)→?
C	⋯	287.56	(C4)→σ^* (C–H)

TABLE III. (*Continued.*)

(b) Peak	E_{exp} (eV)	E_{th} (eV)	Excitation core→final
C	⋯	287.60	(C7)→π^* ethyl
C	⋯	287.62	(C3,5)→σ^* (C–H)
D	⋯	288.69	(C8)→"σ^* (C–C) + ethyl"
D	⋯	288.78	(C7)→?
D	⋯	288.80	(C2,6)→"3π^*"
D	⋯	288.87	(C8)→?
D	⋯	288.88	(C8)→"σ^* (C–C) + ethyl"
D	⋯	288.92	(C4)→"3π^*"
D	⋯	288.97	(C1)→"3π^*"
D	⋯	288.99	(C8)→?
D	⋯	289.00	(C3,5)→"3π^*"

nally, Peak D is characterized by rather diffuse final-state orbitals with mixed σ^* (C–H)/Rydberg and/or 3π^* contributions. The peak region above 287 eV appears also in the experimental NEXAFS spectrum, Fig. 4(A)(a), however, with greatly reduced intensity which will be discussed separately in Sec. IV D.

The experimental spectrum of **ethylbenzene** in Fig. 4(A)(b) shows also a broad asymmetric peak A at about 285.1 eV with some structure at the high-energy side caused by vibrational excitations. A number of peaks with small intensity between 287 and 290 eV are observed. As before, the theoretical NEXAFS spectrum, displayed in Fig. 4(B)(b)

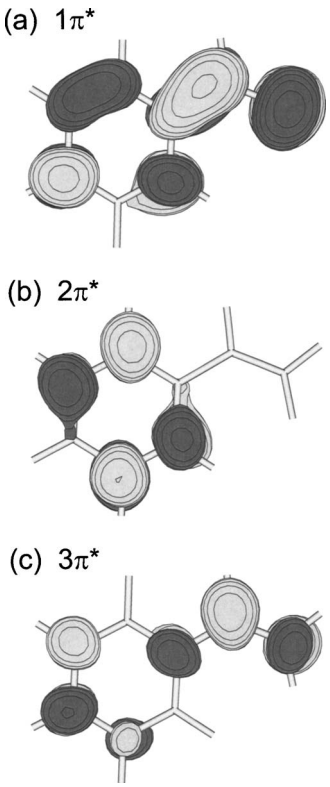

FIG. 5. Constant-value surface plots of final-state orbitals of styrene evaluated for the molecular ground state. (a) 1π^*, (b) 2π^*, and (c) 3π^*. The molecular structure is shown by the bond sticks.

TABLE IV. Comparison of calculated C 1*s* ionization potentials (IP_{calc}) for C_6H_n (n=6, 8, 10, 12) with experimental data (IP_{exp}) (Ref. 40). The absolute uncertainty in the experimental values is estimated to be 0.04 eV. In addition, our calculated IP values for styrene and ethylbenzene are included at the bottom. The theoretical values are obtained from DFT calculations within the ΔSCF approach where relativistic corrections of 0.2 eV are included, see text. Ionized carbon atoms are labeled according to Fig. 1. All values are in eV.

Compound	Ionized C atom	IP_{calc}	IP_{exp}
C_6H_6	1–6	290.13	290.24
1,3-C_6H_8	1, 4	289.77	289.91
	2, 3	290.03	290.12
	5, 6	290.53	290.50
1,4-C_6H_8	1, 2, 4, 5	290.02	290.09
	3, 6	290.58	290.56
C_6H_{10}	1, 2	289.84	289.91
	3, 6	290.36	290.32
	4, 5	290.30	290.26
C_6H_{12}	1–6	290.17	290.12
C_8H_8	1	290.33	···
	2, 4, 6	289.88	···
	3, 5	290.03	···
	7	290.37	···
	8	289.58	···
C_8H_{10}	1	290.05	···
	2, 6	289.82	···
	3, 5	289.94	···
	4	289.87	···
	7	290.48	···
	8	290.32	···

and summarized in Table IIIb, is quite similar to the experimental one. The energetically lowest peak A is assigned to C $1s \rightarrow 1\pi^*$ transitions originating from the carbon atoms of the C_6 ring (C1–C6) where the excitation energies for the chemically nonequivalent carbon atoms differ only by 0.19 eV. Side-chain carbons (C7 and C8) do not contribute to peak A since these atoms are sp^3 hybridized and not connected with the delocalized π system of the C_6 ring. Peaks B–D at higher energies are in their origin quite similar to those of benzene [Fig. 2(B)(a)] with only minor perturbations due to the side chain in ethylbenzene. Peak B is assigned to transitions from all C_6-ring carbon atoms except C1 to final-state orbitals of mixed σ^* (C–C)/Rydberg character. In addition, transitions originating at C8 contribute to peak B where the final-state orbitals are mixtures of the $1\pi^*$ orbital of the C_6 ring and a σ^*-type valence orbital extending over the side chain. This mixture of σ^* and π^* orbitals is possible due to the nonplanar geometry of ethylbenzene. (The side chain is rotated out of the ring plane by 90°.) Peak C is characterized mainly by transitions originating at all carbon atoms of the C_6 ring to final-state orbitals of σ^* (C–H) character with some Rydberg admixture. Finally, peak D contains major contributions from transitions involving the final-state orbital $3\pi^*$ which is similar in its character to the $3\pi^*$ orbital in benzene.

The gray regions and lines in Figs. 2(B) and 4(B) indicate calculated ionization thresholds which are not directly accessible by the present experiments. However, Oltedal *et al.*[46] have recently published experimental atom-resolved IPs for C_6H_n (n=6, 8, 10, 12) molecules. These values are compared in Table IV with our theoretical data obtained from DFT calculations within the Δ self-consistent-field (ΔSCF) approach. Obviously, the agreement is remarkably good, where IP values differ by up to 140 meV only, which may also be due to vibrational corrections.[43] This is further confirmation for the reliability of our theoretical method.

B. Comparison of the spectra

A comparison of the above NEXAFS spectra reveals a number of similarities. All spectra, except those for cyclohexane in Figs. 2(A)(e) and 2(B)(e), are dominated by a rather large peak A appearing at lowest excitation energy about 285 eV which is assigned to transitions of 1*s* electrons at the different double-bonded carbon atoms to unoccupied $1\pi^*$ final-state orbitals. (The absence of C=C double bonds in cyclohexane explains why peak A does not appear in the corresponding spectrum.) The energy position of peak A is quite similar for all molecules, except for 1,3-cyclohexadiene, where it is shifted by 0.6 eV to lower energies compared to the other molecules. The origin of this shift will be discussed in Sec. IV C below. Obviously, the number of C=C double bonds in the C_6 ring of the molecules has no significant effect on the energy position of peak A while nonequivalent carbon atoms of the ring, resulting in energy splitting of $1s \rightarrow 1\pi^*$ transitions, influence the peak width somewhat. Altogether, an intense peak at 285 eV in a NEXAFS spectrum may be taken as a clear fingerprint for a C_6 ring with molecular π^* orbitals similar to those of benzene.

Attaching saturated hydrocarbon chains to the C_6 ring of the molecule does not affect the π system of the ring since the added chains do not offer orbitals which can participate in the π system of the ring. This occurs for ethylbenzene where the coupling is further reduced by the C_2H_5 side chain being rotated by 90° out of the ring plane. In contrast, the π system of unsaturated hydrocarbon side chains which are (close to) planar with respect to the C_6 ring can participate in the π system of the ring resulting in a conjugated system. This leads to shifts and splitting of the lowest excitation energies which can explain broad multipeak structures as found for the $1s \rightarrow 1\pi^*$ transitions of styrene, Figs. 2(A)(a) and 2(B)(a). However, the energy position of the corresponding transitions remains localized at about 285 eV.

The two final-state orbitals of mixed σ^* (C–C)/Rydberg character and mixed σ^* (C–H)/Rydberg character which have been identified recently in the spectrum of benzene,[43] see also Fig. 3 and Table II, can be found in all other molecules considered in this work. While the excitation energies of corresponding C 1*s* core transitions change somewhat due to the nonequivalence of the carbon atoms, transitions involving these final-state orbitals can also be used as fingerprints for C_6-ring structures. Test calculations with polycyclic aromatic molecules, such as naphthalene, indicate that respective final-state orbitals exist also in extended C_6-ring structures. Analogous to our findings for benzene[43] contributions of C

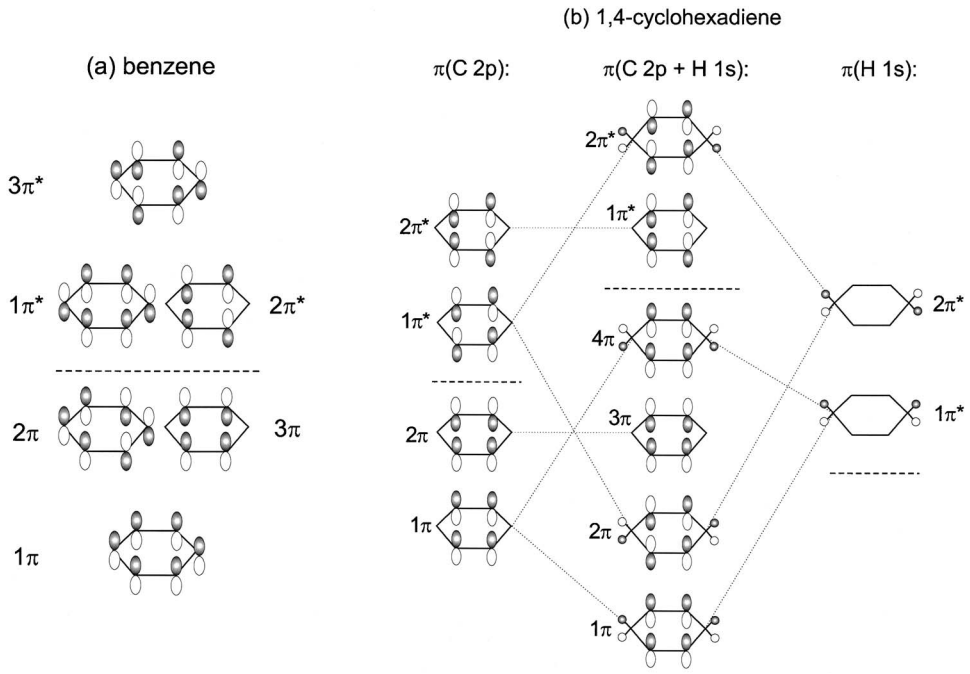

FIG. 6. Schematic drawings of the π-type valence orbitals of (a) benzene and (b) 1,4-cyclohexadiene. The orbital plots are given in qualitative order from bottom (lowest energy) to top (highest energy) where occupied and empty orbitals are separated by a dashed line. For benzene (a) only contributions of the C $2p$ orbitals at CH groups of the C_6 ring are considered (Hückel theory). For 1,4-cyclohexadiene the left part of (b) reflects the orbitals of the Hückel theory approach while the right part shows the two π-type orbitals originating from hydrogen of the two CH_2 groups, see text. The central part of (b) gives a completed orbital scheme with dotted lines indicating orbital hybridization.

$1s$ core excitations to pure (diffuse) Rydberg orbitals are of minor importance for all molecules considered in this work.[47]

C. Low-energy peak A: Comparison of benzene with cyclohexadiene

As mentioned above, peak A in 1,3-cyclohexadiene is shifted to lower energies by 0.6 eV as compared to all other studied molecules except for cyclohexane, where this peak is absent. The origin of this peak shift is not obvious and is connected with the specific π^* orbital structure of this molecule as discussed in the following. We first compare the orbital structure of benzene with that of 1,4-cyclohexadiene, then we describe peculiarities of the orbital structure in 1,3-cyclohexadiene.

In a simple Hückel π electron theory[48] the $2p_z$ orbitals of the six carbon atoms of benzene form six π-type valence orbitals as sketched in Fig. 6(a). Three orbitals are occupied (1π–3π) and three empty ($1\pi^*$–$3\pi^*$). In addition, as a result of the D_{6h} symmetry of C_6H_6 four orbitals form energetically degenerate pairs ($2\pi/3\pi$ and $1\pi^*/2\pi^*$). This orbital structure seems to differ substantially from that of the π electron system of 1,4-cyclohexadiene with a planar C_6 ring where $2p_z$ orbitals of only four carbon atoms, those forming CH groups, contribute as sketched in the left part of Fig. 6(b). However, if the $1s$ orbitals of the four out-of-plane hydrogen atoms referring to the two CH_2 groups of 1,4-cyclohexadiene are included in a π symmetry arrangement [conserving its mirror symmetry, cf. right part of Fig. 6(b)] the extended orbital diagram shown in the central part of Fig. 6(b) corresponds to that of benzene. In this concept, 1,4-cyclohexadiene has six π-type valence orbitals of which four are occupied (1π–4π) and two empty ($1\pi^*$ and $2\pi^*$) in the molecular ground state, as obtained by the theory. [Note that the π occupation of 1,4-cyclohexadiene does not reflect the combined occupation of the two subsystems shown in Fig. 6(b)]. This is explained by changes in the energetic order of σ and π orbitals due to orbital mixing.] Orbitals 1π–3π of 1,4-C_6H_8 and C_6H_6 are equivalent while orbitals $4\pi, 1\pi^*$, and $2\pi^*$ of 1,4-C_6H_8 correspond to $1\pi^*$–$3\pi^*$ of C_6H_6. In particular, the lowest empty orbital $1\pi^*$ of 1,4-cyclohexadiene is very similar in shape with one of the two lowest (degenerate) empty orbitals of benzene, $2\pi^*$. Since these orbitals act as final-state orbitals for C $1s$ core excitations leading to peak A in the corresponding NEXAFS spectra the similarity may rationalize the agreement of the respective excitation energies in the two molecules.

The C_6 ring of 1,3-cyclohexadiene in its ground state is not planar due to the presence of neighboring CH_2 groups in the C_6 ring. As a consequence, the π electron system is formed by $2p_z$ orbitals of the four carbon atoms forming CH groups and being almost coplanar. This yields occupied orbitals $1\pi, 2\pi$ and empty $1\pi^*, 2\pi^*$, as sketched in Fig. 7(a). Due to the missing mirror plane in this molecule the $1s$ or-

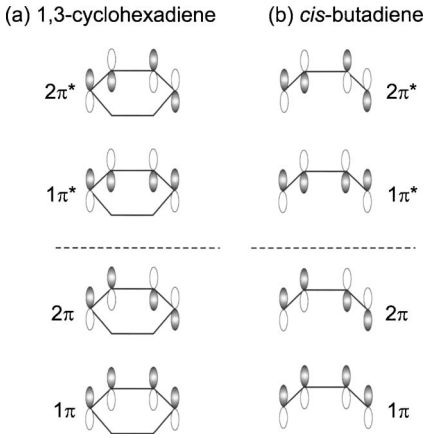

FIG. 7. Schematic drawings of the π-type valence orbitals of (a) 1,3-cyclohexadiene and (b) *cis*-butadiene. The orbital plots are given in qualitative order from bottom (lowest energy) to top (highest energy) where occupied and empty orbitals are separated by a dashed line.

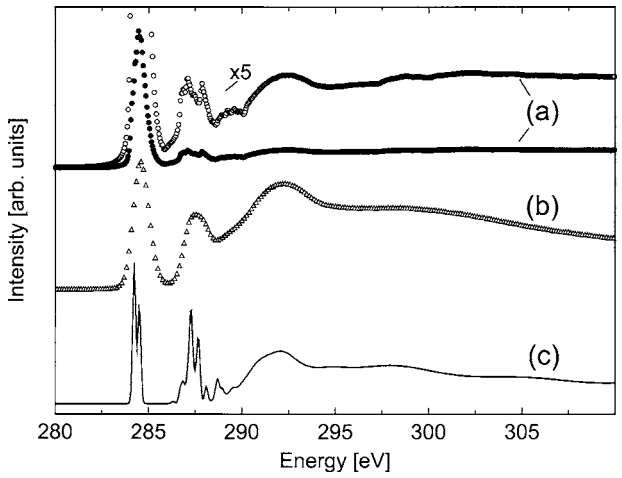

FIG. 8. C 1*s* core excitation spectra of 1,3-cyclohexadiene. (a) Experimental NEXAFS spectrum of this work shown in its original form (full circles) and enlarged by a factor of 5 (open circles). (b) Experimental ISEELS spectrum from the COREX database (Ref. 43). (c) Theoretical NEXAFS spectrum of this work.

bitals of the four hydrogen atoms referring to the two (sp^3 hybridized) CH_2 groups do not contribute to the π electron system as was the case for 1,4-cyclohexadiene. As a result, the valence electron structure of 1,3-cyclohexadiene is quite different in its orbital character from that of 1,4-cyclohexadiene or benzene. In particular, the lowest empty orbital $1\pi^*$ of 1,3-cyclohexadiene does not resemble any of the lowest empty orbitals of benzene, $1\pi^*$ or $2\pi^*$. Since $1\pi^*$ acts as final-state orbital for C 1*s* core excitations determining peak A in the NEXAFS spectrum of 1,3-C_6H_8, the difference with benzene (and with 1,4-C_6H_8) can rationalize the 0.6 eV peak shift mentioned above. However, the actual size of the shift and its direction towards lower energy cannot be explained by simple Hückel theory. Interestingly, a detailed orbital comparison shows that the π electron system of 1,3-cyclohexadiene is quite similar to that of *cis*-butadiene, C_4H_6, whose π orbitals are sketched in Fig. 7(b). This similarity is underlined by the fact that the C $1s \rightarrow 1\pi^*$ excitation in butadiene can also be found at about 284.5 eV,[47] the value obtained for peak A of 1,3-cyclohexadiene. In addition, the transition energy of 287.5 eV for the C $1s \rightarrow 2\pi^*$ excitation of butadiene[47] is also in close correspondence to that of 1,3-cyclohexadiene.

D. NEXAFS intensity at higher energies: 1,3-cyclohexadiene and styrene

Overall, the peak structures of the experimental NEXAFS spectra of all molecules at higher energies above 286 eV are reproduced quite nicely by those of the theoretical spectra with the exception of 1,3-cyclohexadiene and styrene. For the latter two systems, the high-energy peak structure of the present measurements is suppressed substantially compared to theory. The difference between experiment and theory is believed to originate mainly from experimental effects. This is confirmed by previous medium-resolution inner-shell-electron-energy-loss spectra (ISEELS) of gas-phase 1,3-cyclohexadiene[49] shown in Fig. 8 together with theoretical and experimental spectra of the present work. The intensities of our theoretical spectrum agree quite well with those of the previous medium-resolution ISEELS data, shown by the experimental curve (b) in Fig. 8. In addition, the enlargement of the intensity of the present experimental high-resolution NEXAFS spectrum by a factor of 5, given by the open circles (a) in Fig. 8, yields a high-energy peak structure which is also very similar to that of our theoretical spectrum. For styrene the peak structures B–D above 286.5 eV in our theoretical NEXAFS spectrum shown in Fig. 4(B)(a) are also largely suppressed in the present experimental spectrum of Fig. 4(A)(a). However, the intensities of our theoretical NEXAFS spectrum agree again quite well with those of a medium-resolution spectrum measured for multilayers of styrene.[45] Here the comparison with condensed styrene seems appropriate since the corresponding final-state orbitals of the molecule are of dominant valence character. This is analogous to condensed and gas-phase benzene where both NEXAFS spectra are quite similar.[50]

An unambiguous explanation of the peak suppression in the experiment cannot be offered at this point. One could speculate about different possibilities where we mention only two. First, the theory calculates photoabsorption cross sections while in the experiment the total photoionization yield, i.e., the number of charged particles created in a decay process subsequent to the excitation, is detected. A comparison of the two quantities is adequate only if the average number of Auger electrons created in the decay process is independent of the photon energy. While no significant influence on NEXAFS spectra caused by this effect has been found in earlier studies on a large number of other molecules, see, for example, Ref. 40, an energy-dependent yield of Auger electrons in styrene and 1,3-cyclohexadiene might explain the observed result. Possibly, the molecules in their excited $1\pi^*$ states emit Auger cascades of many slow electrons whereas higher excited states result in emission of only a few fast Auger electrons. Here, possible differences would be in line with formation of different photofragments. Unfortunately, no detailed information concerning Auger decays of resonantly excited small organic molecules has been published so far. Second, in the experimental setup, the angular distribution of emitted Auger electrons may depend on the molecule and the excited state, since the stainless-steel plate of the detector does not cover a full detection angle of 4π. This might partly explain the differences between experiment and theory and can be checked by comparing data of different detector geometries, which has not been done so far. The two experimental problems described above can arise in the NEXAFS spectra of all molecules considered in this work but seem to be most pronounced for 1,3-cyclohexadiene and styrene. It should be noted that the excitation spectrum resulting from ISEELS experiments on 1,3-cyclohexadiene,[49] see Fig. 8, is not expected to be affected by these problems.

Altogether, our theoretical NEXAFS spectra describe the peak positions observed in the present high-resolution spectra quite well, although the intensities are quenched at higher energies. This effect does not seem to appear in the medium-resolution ISEELS and solid-state NEXAFS spectra.[45,49]

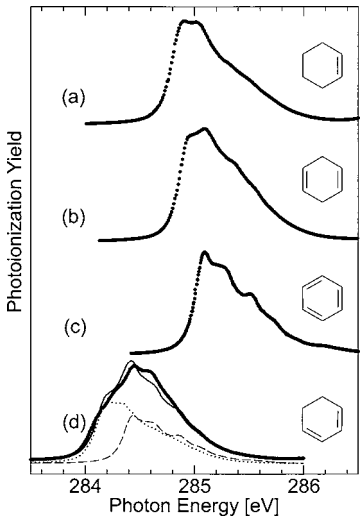

FIG. 9. Experimental spectra of C $1s \rightarrow \pi^*$ transitions (peaks A in Fig. 2) for (a) cyclohexene, (b) 1,4-cyclohexadiene, (c) benzene, and (d) 1,3-cyclohexadiene. The thin solid line in (d) represents the total "theoretical" spectrum given by an intensity-weighted superposition of spectra (b) and (c) using the approach described in the text.

E. Vibrational analysis

Peak positions and most intensities of the measured NEXAFS spectra are described quite well by our theoretical spectra. However, all peaks in the experimental spectra are broadened asymmetrically due to additional vibrational fine structure. While a consistent theoretical treatment of vibrational coupling during the core excitation process is rather difficult and has been considered only for few molecular systems such as pyridine,[40] we can rationalize the qualitative effect by a simple C–C neighbor binding scheme. Here it is assumed that vibrational coupling of the core excitation and corresponding peak broadening is determined by the local binding environment of the carbon atom where the core hole is created. This will be illustrated for the observed vibrational progressions of the low-energy peak A of C_6H_6, C_6H_8, and C_6H_{10}, see Fig. 2, which has been assigned to C $1s \rightarrow 1\pi^*$ excitations.

Figure 9 shows the spectral region around peak A in Fig. 2 for (a) cyclohexene, (b) 1,4-cyclohexadiene, (c) benzene, and (d) 1,3 cyclohexadiene in greater detail, where vibrational fine structure on the high-energy side of the peaks becomes evident. Obviously, the shape of peak A is almost identical for cyclohexene and 1,4-cyclohexadiene, suggesting similar geometric changes due to electronic core excitations. This can be understood by details of the binding environment. In these two molecules the carbon atoms where the excitations determining peak A originate, i.e., C1, C2, C4, and C5 for 1,4-cyclohexadiene and C1 and C2 for cyclohexene [Figs. 1(c) and 1(d)], all see the same carbon binding environment, labeled e_1 in the following. They couple with one nearest carbon neighbor by a C–C double bond, where the neighbor itself forms both a single and a double C–C bond with its neighbors, and with the other nearest neighbor by a C–C single bond, where the neighbor itself sees two single C–C bonds. This carbon binding environment e_1, common to cyclohexene and 1,4-cyclohexadiene, could explain the identical vibrational progression on the right side of peak A observed for the two molecules, see Figs. 9(a) and 9(b). In contrast, the carbon atoms of benzene, C1–C6 in Fig. 1(a), which all contribute to peak A, see a carbon binding environment e_2, which differs from e_1. Here each carbon couples with one nearest carbon neighbor by a C–C double bond and with the other by a C–C single bond where both neighbors themselves form a single and a double C–C bond with their neighbors. As a result of the different binding environment the vibrational progression of peak A for benzene is expected to vary from that of the former two molecules. This is confirmed by the experiment where the vibrational progression on the right side of peak A, see Fig. 9(c), decays more rapidly and exhibits a pronounced structure compared to the curves in Figs. 9(a) and 9(b).

The 1,3-cyclohexadiene molecule differs from those discussed above in that it contains carbon atoms with two types of binding environments, e_1 for C1 and C4 and e_2 for C2 and C3. In the theoretical NEXAFS spectrum of this molecule peak A is split into two components A′ at lower and A″ at higher energies where peak A′ refers to C $1s \rightarrow 1\pi^*$ excitations originating at C1 and C4 while peak A″ is determined by those at C2 and C3. Thus, in an approximate theoretical treatment of vibrational broadening peak A′ should be associated with vibrational structure referring to environment e_1 and A″ with that of environment e_2. This idea has been used to evaluate a total "theoretical" peak A for 1,3-cyclohexadiene in analogy to a procedure described in Ref. 46. Here the experimental peak A for cyclohexene [Fig. 9(a)], simulating an e_1-type vibrational progression, is placed at the theoretical excitation energy of peak A′ [dotted line in Fig. 9(d)] and the experimental peak A for benzene [Fig. 9(c)], simulating an e_2-type vibrational progression, at the theoretical energy of peak A″ (dashed line in Fig. 9(d)]. The superposition of the two peaks with relative weights reflecting the theoretical intensity ratio of peaks A′ and A″ yields a broad peak shown as a thin line in Fig. 9(d) which comes rather close to the experimental shape of peak A [thick line in Fig. 9(d)] considering the simplicity of the approach. In particular, detailed molecular tension in the C_6 ring of the molecules is not included in the present treatment.

The application of the present model of vibrational broadening to the two larger molecules, ethylbenzene and styrene, is more involved due to the increased complexity of binding environments. In these molecules carbon atoms C3–C5, see Figs. 1(f) and 1(g), experience e_1-type binding environments. Thus, corresponding C $1s \rightarrow 1\pi^*$ transitions contributing to peak A for ethylbenzene and styrene are expected to behave similar to those of benzene concerning vibrational broadening. However, the central carbon C1 in the two molecules sees a binding environment e_3 dominated by its three carbon neighbors and being substantially different from both e_1 and e_2 which must affect the corresponding vibrational fine structure. Therefore, a simulation of a total theoretical peak A for these molecules according to our approach must include an experimental reference spectrum with vibrational structure emphasizing the e_3-type binding environment. This does not seem to exist so far which prevents the application of our approach.

V. CONCLUSIONS

The present experimental high-resolution NEXAFS spectra for small C_6-ring-containing organic molecules near the C 1*s* ionization threshold are found to agree quite well with our theoretical spectra from state-of-the-art DFT calculations. This allows a consistent interpretation of spectral details in terms of underlying excitation processes. The spectral features are determined mainly by electronic transitions from C 1*s* core to different π^*-type final-state orbitals, while transitions to σ^*-type final-state orbitals, of strong valence character with small admixture of Rydberg contributions, contribute less. Further, transitions to pure Rydberg-type final-state orbitals can be neglected in the spectra. The C 1*s* ionization spectrum of benzene is quite simple due to the equivalence of the carbon atoms in the C_6 ring. In contrast, the other molecules, except cyclohexane, contain different nonequivalent carbon atoms, which leads to energy splittings of the different excitations yielding more complex spectra.

All NEXAFS spectra, except that of cyclohexane, exhibit a strong low-energy peak A near 285 eV which our theoretical analysis assigns to transitions of 1*s* electrons at the different double-bonded carbon atoms to unoccupied $1\pi^*$ final-state orbitals. The absence of C=C double bonds in cyclohexane explains why the low-energy peak does not appear in the corresponding spectrum. The excitation energy of peak A is very similar for all molecules, except for 1,3-cyclohexadiene where it is shifted by 0.6 eV to lower energies. This is explained by the different shapes of the unoccupied $1\pi^*$ final-state orbitals where the $1\pi^*$ orbital of 1,3 cyclohexadiene differs substantially from those of the other molecules and is very similar to that for *cis*-butadiene. In contrast, $1\pi^*$ orbitals of the other molecules are rather similar in shape and result in almost identical excitation energies. This indicates that the energy position of the C $1s \rightarrow 1\pi^*$ transition depends less on the extent of delocalization of the π electrons but more on the local binding environment of the carbon atom where the excitation originates. Adding saturated side chains to the C_6 ring of the molecule does not affect the excitation energy of the C $1s \rightarrow 1\pi^*$ transition, as found for ethylbenzene. In contrast, additional unsaturated side chains can interact with the π system of the ring leading to orbital mixing of the ring and the side chains. This may result in slightly changed excitation energies and additional peaks near peak A as confirmed by the experimental and theoretical spectra of styrene. Nevertheless, this is not a major factor, because the energy position of the corresponding transition remains localized at about 285 eV, in close correspondence to benzene.

Apart from the C $1s \rightarrow 1\pi^*$ transitions observed in the NEXAFS spectra of the present molecules other final-state orbitals have been identified, which can also act as characteristics of the C_6-ring structures. These orbitals are of mixed σ^* (C–C)/Rydberg or σ^* (C–H)/Rydberg character and corresponding excitations are found in all molecules of the present study with energies depending slightly on the system.

The experimental NEXAFS spectra are of sufficient resolution to reveal vibrational fine structure. Unfortunately, a consistent theoretical treatment of vibrational coupling during the core excitation process is rather difficult and has not been taken into account in our present theory. However, vibrational fine structure can become important in the comparison of the theoretical and experimental spectra. Examples are molecules with close-lying electronic excitations, where the superimposed vibrational structure can lead to considerable differences in intensity ratios between experiment and theory ignoring vibrational coupling.[40] This applies also to those molecules of the present study where nonequivalent carbon atoms affect the C $1s \rightarrow 1\pi^*$ transitions. Here we propose an approximate treatment of vibrational coupling combining theoretical results for the electronic transitions with experimental information concerning the vibrational progression. For a given molecule each carbon atom which acts as an excitation center is classified with respect to its binding environment. The vibrational structure of this core excitation is then assumed to agree with that of a carbon atom in the same binding environment in a different molecule where the excitation is energetically well separated. Combining the vibrational progression from corresponding experimental NEXAFS spectra for all atoms with different binding environment in a molecule with corresponding theoretical energy positions and intensity ratios leads to a simulated spectrum. For 1,3-cyclohexadiene this procedure is found to yield very good agreement with the experimental NEXAFS spectrum, analogous to previous findings for pyridine.[40] This may suggest that vibrational structure in NEXAFS spectra referring to specific atoms in a certain local binding environment can be transferred and superimposed to yield the complete spectrum. Nevertheless, there is a huge demand for further theoretical studies on the vibrational fine structure of core-excited molecules. Furthermore, from the experimental side more advanced studies such as resonant Auger and photofragmentation studies are necessary to understand the dynamic of the photofragmentation process in more detail.

ACKNOWLEDGMENTS

This work is dedicated to Professor Volker Staemmler in honor of his 65th birthday. This work has been supported by Deutsche Forschungsgemeinschaft (DFG) through Sonderforschungsbereich 546 "Transition Metal Oxide Aggregates" and DFG-Project No. PU 180/2-1. Further, experimental support by W. Stolte is gratefully acknowledged. We would like to thank the ALS staff for providing excellent working conditions. Part of this work was supported by the Department of Energy, Office of Science, Basic Energy Sciences, Chemical Sciences Division. The Advanced Light Source is supported by the Department of Energy, Materials Sciences Division.

[1] H. Oji, R. Mitsumoto, E. Ito, H. Ishii, Y. Ouchi, K. Seki, T. Yokoyama, T. Ohta, and N. Kosugi, J. Chem. Phys. **109**, 10409 (1998).
[2] R. Püttner, M. Domke, and G. Kaindl, Phys. Rev. A **57**, 297 (1998).
[3] L. Yang, O. Plachkevytch, H. Ågren, and L. G. M. Pettersson, J. Phys. IV **7**, 227 (1997).
[4] A. P. Hitchcock, D. C. Newbury, I. Ishii, J. Stöhr, J. A. Horsley, R. D. Redwing, A. L. Johnson, and F. Sette, J. Chem. Phys. **85**, 4849 (1986).
[5] P. Väterlein, M. Schmelzer, J. Taborski, T. Krause, F. Viczian, M. Bässler, R. Fink, E. Umbach, and W. Wurth, Surf. Sci. **452**, 20 (2000).
[6] S. Reiss, H. Krumm, A. Niklewski, V. Staemmler, and C. Wöll, J. Chem. Phys. **116**, 7704 (2002).

[7] L. G. M. Pettersson, H. Ågren, Y. Luo, and L. Triguero, Surf. Sci. **408**, 1 (1998).
[8] F. Matsui, H. W. Yeom, I. Matsuda, and T. Ohta, Phys. Rev. B **62**, 5036 (2000).
[9] J. G. Chen, Surf. Sci. Rep. **30**, 5 (1997).
[10] L. Soriano, M. Abbate, J. C. Fuggle, M. A. Jimenez, J. M. Sanz, C. Mythen, and H. A. Padmore, Solid State Commun. **87**, 699 (1993).
[11] R. Radhakrishnan, C. Reed, S. T. Oyama, M. Seman, J. N. Kondo, K. Domen, Y. Ohminami, and K. Asakura, J. Phys. Chem. B **105**, 8519 (2001).
[12] J. Böse, A. Osanna, C. Jacobsen, and J. Kirz, J. Electron Spectrosc. Relat. Phenom. **85**, 9 (1997).
[13] K. Kaznacheyev, A. Osanna, C. Jacobsen, O. Plashkevych, O. Vahtras, and H. Ågren, J. Phys. Chem. A **106**, 3153 (2002).
[14] S. G. Urquhart, A. P. Hitchcock, A. P. Smith, H. W. Ade, W. Lidy, E. G. Rightor, and G. E. Mitchell, J. Electron Spectrosc. Relat. Phenom. **100**, 119 (1999).
[15] S. G. Urquhart, A. P. Hitchcock, R. D. Priester, and E. G. Rightor, J. Polym. Sci., Part B: Polym. Phys. **33**, 1603 (1995).
[16] A. P. Hitchcock, J. Synchrotron Radiat. **8**, 66 (2001).
[17] H. Ågren, V. Carravetta, L. G. M. Pettersson, and O. Vahtras, Physica B **209**, 477 (1995).
[18] L. G. M. Pettersson, H. Ågren, B. L. Schurmann, A. Lippitz, and W. E. S. Unger, Int. J. Quantum Chem. **63**, 749 (1997).
[19] O. Plashkevych, L. Yang, O. Vahtras, H. Ågren, and L. G. M. Pettersson, Chem. Phys. **222**, 125 (1997).
[20] T. Okajima, K. Teramoto, R. Mitsumoto, H. Oji, Y. Yamamoto, I. Mori, H. Ishii, Y. Ouchi, and K. Seki, J. Phys. Chem. A **102**, 7093 (1998).
[21] R. N. S. Sodhi and C. E. Brion, J. Electron Spectrosc. Relat. Phenom. **34**, 363 (1984).
[22] B. Hammer, L. B. Hansen, and J. K. Nørskov, Phys. Rev. B **59**, 7413 (1999).
[23] J. P. Perdew, K. Burke, and M. Ernzerhof, Phys. Rev. Lett. **77**, 3865 (1996).
[24] K. Hermann and L. G. M. Pettersson, program package StoBe (Stockholm, Berlin, 2005), a modified version of the DFT-LCGTO program package deMon by A. St.-Amant and D. Salahub (University of Montreal).
[25] T. H. Dunning, J. Chem. Phys. **55**, 716 (1971).
[26] S. Huzinaga, J. Chem. Phys. **42**, 1293 (1965).
[27] W. Kutzelnigg, U. Fleischer, and M. Schindler, *NMR-Basic Principles and Progress* (Springer, Heidelberg, 1990), Vol. 23, p. 165.
[28] A. Mattsson, I. Panas, P. Siegbahn, U. Wahlgren, and H. Åkeby, Phys. Rev. B **36**, 7389 (1987).
[29] L. G. M. Pettersson, U. Wahlgren, and O. Gropen, Chem. Phys. **80**, 7 (1983).
[30] N. Kosugi, Chem. Phys. **289**, 117 (2003).
[31] A. B. Rocha and C. E. Bielschowsky, J. Chem. Phys. **113**, 7971 (2000).
[32] R. F. Fink, S. L. Sorensen, A. N. de Brito, A. Ausmees, and S. Svensson, J. Chem. Phys. **112**, 6666 (2000).
[33] N. V. Dobrodey, H. Koppel, and L. S. Cederbaum, Phys. Rev. A **60**, 1988 (1999).
[34] H. Ågren, V. Carravetta, O. Vahtras, and L. G. M. Pettersson, Theor. Chem. Acc. **97**, 14 (1997).
[35] See EPAPS Document No. E-JCPSA6-123-015546 for the equilibrium geometries of all molecules in Cartesian coordinates given in angstrom units. This document can be reached via a direct link in the online article's HTML reference section or via the EPAPS homepage (http://www.aip.org/pupservs/epaps.html).
[36] J. C. Cochran, K. Hagen, G. Paulen, Q. Shen, S. Tom, M. Traetteberg, and C. Wells, J. Mol. Struct. **413**, 313 (1997).
[37] J. C. Slater, in *Advances in Quantum Chemistry*, edited by P. O. Loewdin (Academic, New York, 1972), p. 1.
[38] J. C. Slater and K. H. Johnson, Phys. Rev. B **5**, 844 (1972).
[39] L. Triguero, O. Plashkevych, L. G. M. Pettersson, and H. Agren, J. Electron Spectrosc. Relat. Phenom. **104**, 195 (1999).
[40] C. Kolczewski, R. Püttner, O. Plashkevych, *et al.* J. Chem. Phys. **115**, 6426 (2001).
[41] T. Privalov, O. Plashkevych, F. Gel'mukhanov, and H. Ågren, J. Chem. Phys. **113**, 3734 (2000).
[42] O. Plashkevych, H. Ågren, V. Carravetta, G. Contini, and G. Polzonetti, Chem. Phys. Lett. **327**, 7 (2000).
[43] R. Püttner, C. Kolczewski, M. Martins, A. S. Schlachter, G. Snell, M. Sant'Anna, J. Viefhaus, K. Hermann, and G. Kaindl, Chem. Phys. Lett. **393**, 361 (2004).
[44] K. Ueda, M. Okunishi, H. Chiba, Y. Shimizu, K. Ohmori, Y. Sato, E. Shigemasa, and N. Kosugi, Chem. Phys. Lett. **236**, 311 (1995)
[45] M. Wühn, Y. Joseph, P. S. Bagus, A. Niklewski, R. Püttner, S. Reiss, W. Weiss, M. Martins, G. Kaindl, and C. Wöll, J. Phys. Chem. B **104**, 7694 (2000).
[46] V. M. Oltedal, K. J. Børve, L. J. Sæthre, T. D. Thomas, J. D. Bozek, and E. Kukk, Phys. Chem. Chem. Phys. **6**, 4254 (2004).
[47] J. Stöhr, in *NEXAFS Spectroscopy*, Springer Series in Surface Sciences Vol. 25, edited by G. Ertl, R. Gomer, and D. L. Mills (Springer, Heidelberg, 1992).
[48] See, e.g., W. Kutzelnigg, *Einführung in die Theoretische Chemie* (Wiley-VCH, Weinheim, 2001).
[49] COREX database of atomic and molecular core edge excitation oscillator strengths, as described by A. P. Hitchcock and D. C. Mancini, J. Electron Spectrosc. Relat. Phenom. **67**, 1 (1994); see also http://unicorn.mcmaster.ca/corex/alpha-list.html
[50] D. Menzel, G. Rocker, H. P. Steinrück, D. Coulman, P. A. Heimann, W. Huber, P. Zebisch, and D. R. Lloyd, J. Chem. Phys. **96**, 1724 (1992).